Progress In Electromagnetics Research Letters, Vol. 60, 45–51, 2016

Analysis of Wide Band Scattering from Objects Using the Adaptive Improved Ultra-Wide Band Characteristic Basis Functions

Wen-Yan Nie[1] and Zhong-Gen Wang[2, *]

Abstract—The improved ultra-wide band characteristic basis function method (IUCBFM) is an efficient approach to analyze the wide-band scattering problems because the improved ultra-wide characteristic basis functions (IUCBFs) can be reused for any frequency sample in the range of interest. However, the number of the IUCBFs constructed at the highest frequency point is excessive, and the computational complexity will be increased when applying the same number of IUCBFs at the lower frequency points. To mitigate this problem, an adaptive IUCBFs construction method is presented which can decrease the computational complexity at the lower frequency points. In the proposed method, the given frequency band is adaptively divided into multiple sub-bands in consideration of the number of the IUCBFs. The adaptive IUCBFs are obtained at the highest frequency point in each sub-band, which leads to smaller number of IUCBFs and significant reduction of solver time at lower frequency band. The numerical results have demonstrated the accuracy and efficiency of the proposed method.

1. INTRODUCTION

Accurate prediction of the wideband radar cross section (RCS) of objects has great significance in the studies of high-resolution radar imaging technology, anti-stealth and target identification. One of the most popular methods for RCS prediction is the frequency domain integral equation solved using method of moments (MoM) [1]; however, it places a heavy burden on the CPU time as well as on memory requirements when electrically large structures are analyzed. Moreover, in order to obtain the RCS over a wide frequency band using MoM, the calculation at each frequency point has to be repeated over the band of interest which increases computational time. A number of efficient methods, such as the fast multipole method (FMM) [2], multilevel fast multipole method (MLFMM) [3, 4], adaptive integration method (AIM) [5], adaptive cross approximation (ACA) algorithm [6], and characteristic basis function method (CBFM) [7, 8], have been proposed to improve the calculation efficiency at single frequency point. However, if the RCS is highly frequency dependent, then the calculations are required to be performed at finer increment of frequency to obtain an accurate representation of the frequency response which is computationally intensive. Recently, several techniques have been proposed to circumvent this problem. In [9], the model-based parameter estimation (MBPE) is used to obtain the wide-band data from frequency and frequency-derivative data. In [10], the impedance matrix is computed at relatively large frequency intervals and then interpolated to approximate its values. However, all the above mentioned methods still rely on an iteration method to solve the linear equations that usually faces unpredictable problems of convergence rate. In [11, 12], the asymptotic waveform evaluation (AWE) technology has been used to analyze the wide-band electromagnetic scattering problems and has achieved good results but this technology needs to store dense impedance matrixes and their frequency

Received 30 March 2016, Accepted 10 May 2016, Scheduled 13 May 2016
* Corresponding author: Zhong-Gen Wang (zgwang@ahu.edu.cn).
[1] College of Mechanical and Electrical Engineering, Huainan Normal University, Huainan, Anhui 232001, China. [2] College of Electrical and Information Engineering, Anhui University of Science and Technology, Huainan, Anhui 232001, China.

derivatives, which enlarges the memory requirement. So in [13], the AWE based on the CBFM, is proposed to analyze the wide-band electromagnetic scattering problems. An adaptive modified CBFM combined with the MBPE technology is proposed in [14] to analyze the wide-band and wide-angle electromagnetic scattering problems. Although the above mentioned two methods utilize the CBFM to accelerate solving speed of the interpolation point and to reduce memory consumption, both the methods need to recalculate the characteristic basis functions (CBFs) at each interpolation point. Hence, in [15], an ultra-wide band CBFM (UCBFM) is proposed to analyze the wide-band electromagnetic scattering problems without having the requirement to repeatedly construct the CBFs at each frequency. The CBFs constructed at the highest frequency point, termed ultra-wide band CBFs (UCBFs), entail the electromagnetic behavior at lower frequency range; thus, it implies that they can also be employed at lower frequency points without going through the time consuming step of reconstruction. However, the errors of the RCS calculated by the UCBFs are usually large at lower frequency points because of weak universality of the UCBFs. In [16], the construction of the UCBFs is improved by considering the CBFs constructed at the lowest frequency point. An improved UCBFM (IUCBFM) is presented in [17]. This method fully considers the mutual coupling effects among the sub-blocks to obtain the secondary level CBFs (SCBFs) with a stronger universality, such that the improved UCBFs (IUCBFs) contain more current information, and to improve the calculation accuracy at lower frequency points. Although the accuracy of the above methods is improved, it should be noted that the number of IUCBFs is unnecessarily high and that the computational complexity will be increased when applying the IUCBFs to the lower frequency points. In this paper, an adaptive IUCBFM (AIUCBFM) is presented. The proposed method adaptively divides the given frequency band into multiple sub-bands keeping the number of the IUCBFs under consideration, which leads to smaller number of IUCBFs at the lower sub-frequency band. The RCS data are then calculated utilizing the IUCBFs obtained at the highest frequency point in each sub-band. The smaller number of IUCBFs results in a substantial time-saving in the fill procedure of the reduced matrix at the lower frequencies. Finally, the wide RCS data over the given frequency band are obtained by splicing the RCS data in each frequency band.

This paper is composed of the following sections. The next section describes the IUCBFM. In Section 3, the AIUCBFM is described. Section 4 presents the numerical results for three test targets to demonstrate that the AIUCBFM is accurate and efficient. In Section 5, the paper is concluded.

2. IMPROVED ULTRA-WIDE BAND CHARACTERISTIC BASIS FUNCTION METHOD

The IUCBFM [17] firstly divides the object into M blocks. Then, it establishes a model at the highest frequency point f_h. The multi-angle plane wave excitations are set to irradiate each block. Assume that the numbers of plane wave excitations in directions of θ and ϕ are N_θ and N_ϕ, respectively. For each plane wave excitation, the primary CBFs (PCBFs) of block i can be solved by the following formula:

$$\mathbf{Z}_{ii}\mathbf{J}_i^P = \mathbf{E}_i, \tag{1}$$

where, $\mathrm{E}_{\mathbf{i}}$ represents the excitation vector of block i, for$i = 1, 2, 3 \cdots M$; $\mathbf{Z}_{ii}$ represents the self-impedance of block i, with dimensionality of $N_i \times N_i$, and $\mathbf{J}_i^P$ is the PCBFs matrix of dimension $N_i \times 1$. After the PCBFs of each block are solved, according to Foldy-Lax equation theory [18, 19], the SCBFs on each block are calculated by replacing the incident field with the scattered fields due to the PCBFs on all blocks except from itself. By solving Eq. (2), the first-level SCBFs can be obtained. Similarly, the higher-level SCBFs can be calculated if the second-level SCBFs is calculated, and these SCBFs can be calculated as

$$\mathbf{Z}_{ii}\mathbf{J}_i^{S1} = -\sum_{j=1(j\neq i)}^{M} \mathbf{Z}_{ij}\mathbf{J}_j^P, \tag{2}$$

$$\mathbf{Z}_{ii}\mathbf{J}_i^{S2} = -\sum_{j=1(j\neq i)}^{M} \mathbf{Z}_{ij}\mathbf{J}_j^{S1}. \tag{3}$$

By solving Eqs. (2) and (3), $6N_\theta N_\phi$ CBFs can be obtained by considering θ-and ϕ -polarizations (including $2N_\theta N_\phi \mathbf{J}^P$, $2N_\theta N_\phi \mathbf{J}^{S1}$ and $2N_\theta N_\phi \mathbf{J}^{S2}$). Typically, the number of plane waves used to generate the CBFs will exceed the number of degrees of freedom associated with the block. To reduce the linear dependency among these CBFs, an orthogonalization procedure based on the singular value decomposition (SVD) method is used to reduce the final number of CBFs. Only those relative singular values above a certain threshold, for example 1.0E-3, are retained as the IUCBFs. Assuming that there are K IUCBFs retained on each block after SVD, the surface current can be expressed as a liner combination of the IUCBFs as follows:

$$\mathbf{J} = \sum_{m=1}^{M} \sum_{k=1}^{K} \alpha_m^k(f) J_m^{CBF_k}, \tag{4}$$

where, $J_m^{CBF_k}$ represents the kth IUCBFs of block$m$, and $\alpha_m^k(f)$ represents the unknown weight coefficients. The Galerkin method [7, 8] is used to convert the traditional MoM equation into a linear equation relating the coefficient matrix $\alpha(f)$. A $KM \times KM$ reduced matrix can be obtained:

$$\mathbf{Z}^{\mathbf{R}}(f) \cdot \alpha(f) = \mathbf{V}^{\mathbf{R}}(f), \tag{5}$$

where, $V_i^R(f) = \mathbf{J}^T \cdot \mathbf{E}_i(f)$, and T represents the transposition. $\mathbf{Z}^{\mathbf{R}}(f)$ represents the reduced impedance matrix of dimension $KM \times KM$. Its detailed calculation expression can be expressed as below:

$$Z_{ij}^R(f) = \mathbf{J}^{\mathrm{T}} \cdot \mathbf{Z}_{ij}(f) \cdot \mathbf{J} \quad i, j \leq M. \tag{6}$$

where, $\mathbf{Z}_{ij}(f)$ represents the impedance matrix between i and j blocks. Because the dimensionality of $\mathbf{Z}^{\mathbf{R}}(f)$ is small, $\alpha(f)$ can be obtained by directly solving Eq. (5). Then, $\alpha(f)$ is substituted into Eq. (4). In this way, the surface current at any frequency point can be obtained. The construction of the IUCBFs fully considers the mutual coupling effects among the sub-blocks, which not only enables the IUCBFs to contain more current information characteristics, but also greatly decreases the number of plane wave excitations. Although the IUCBFs can be reused at each frequency point, it should be noted that the number of IUCBFs constructed at the highest frequency point is greater than the IUCBFs constructed at the lower frequency points. If the number of IUCBFs is the same over the entire frequency band, then the computational complexity of the reduced impedance matrix construction at the lower frequency points will be increased.

3. ADAPTIVE CONSTRUCTION OF IMPROVED ULTRA-WIDE BAND CHARACTERISTIC BASIS FUNCTIONS

An adaptive construction of the IUCBFs is presented in this paper to decrease the computational complexity at the lower frequency points. In the proposed method, the given frequency band is adaptively divided into multiple sub-bands in consideration of the IUCBFs number, and the adaptive IUCBFs (AIUCBFs) can be obtained at the highest frequency point in each sub-band. Then, the wide-band RCS of each sub-band is calculated utilizing the AIUCBFs generated at the corresponding sub-band. Finally, the whole RCS data of the given frequency band can be obtained by splicing the RCS data of each frequency sub-band. For a given frequency band $[f_{\min}, f_{\max}]$, the AIUCBFs can be obtained through the following steps:

Step 1: Setting the initial frequency point $f_L = f_{\min}$ and $f_H = f_{\max}$;

Step 2: Separately constructing the IUCBFs at frequency point$f_H$andf_L. Suppose that the total numbers of IUCBFs at f_H and f_L are K_H and K_L, respectively.

Step 3: Defining ε as a threshold level ($0 < \varepsilon \leq 1$ typically chosen to be 0.5), if $K_L/K_H > \varepsilon$, the IUCBFs constructed at f_H can be reused in the entire frequency band, else take $f_{mid} = (f_H + f_L)/2$, repeat step 2 in $[f_L, f_{mid}]$ and $[f_{mid}, f_H]$ until $K_L/K_H > \varepsilon$.

The obtained AIUCBFs are constructed at the highest frequency point in each sub-band. Compared to the IUCBFs constructed by using the IUCBFM, the number of AIUCBFs is smaller, so the fill process of the reduced impedance matrix can be speeded up.

4. NUMERICAL RESULTS

To verify the validity and accuracy of the AIUCBFM, the results for the scattering problem are presented using a perfectly electric conducting (PEC) plate, a PEC sphere and a PEC cube. All the simulations are performed using only one core of a personal computer with an Intel(R) Pentium(R) G2030 CPU with 3.0 GHz and 4 GB RAM. The second-level of the SCBFs is calculated, the ε set to 0.5 and the threshold of SVD set to 0.001.

First, the scattering problem of a PEC plate with side length of 0.2 m over a frequency range of 0.1 GHz to 3 GHz is considered. The geometry is divided into 1628 triangular patches with an average length of $\lambda/10$ at 3 GHz which leads to 3184 unknowns. The geometry is divided into 4 blocks, with each block extended by $\Delta = 0.15\lambda$ in all directions. Referring to [17], the IUCBFs are constructed for the IUCBFM. 8 plane wave excitations in directions of θ and ϕ are set and 51 IUCBFs retained on each block after the SVD. The total number of IUCBFs retained after the SVD at each frequency point is shown in Fig. 1. It can be seen that the number of IUCBFs constructed at the highest frequency point is greater than the IUCBFs constructed at the lower frequency points. The same number of IUCBFs over the entire frequency band will increase the computational complexity at the lower frequency points. In AIUCBFM, the given frequency band is adaptively divided into 4 sub-bands. The broadband RCS (10 frequency sampling points in each sub-band) is obtained by using the IUCBFM and the AIUCBFM over a frequency range of 0.3 GHz to 3 GHz and shown in Fig. 2. The results calculated by using the AIUCBFM agree well with the that obtained by the IUCBFM. Table 1 lists the number of IUCBFs and CPU time of the two methods. It can be seen that the number of IUCBFs at lower frequency band derived by using the AIUCBFM is evidently smaller than that obtained using the IUCBFM and thus leads to accelerating the fill procedure of the reduced matrix at lower frequency points.

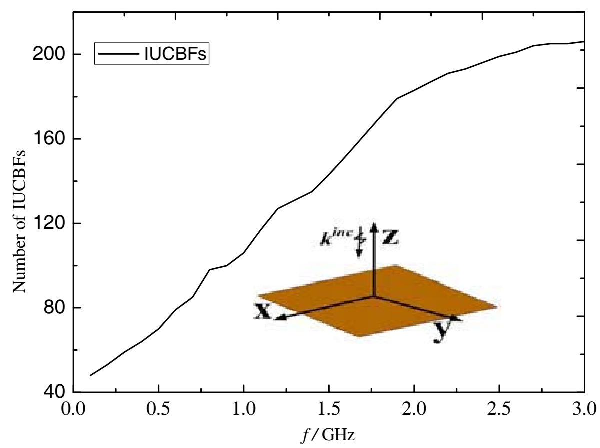

Figure 1. The number of IUCBFs at each frequency point.

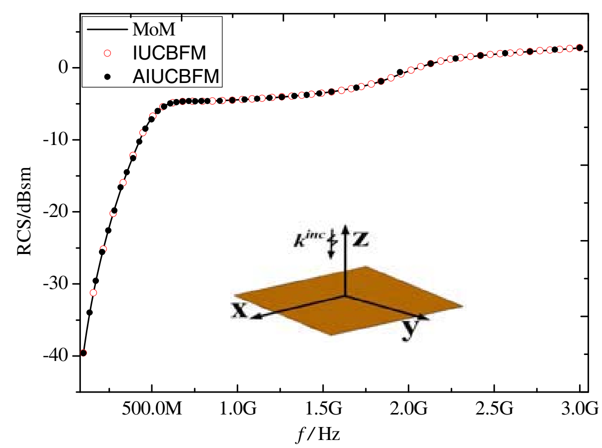

Figure 2. Broadband RCS of the PEC plate.

Table 1. Number of IUCBFs and the CPU time of IUCBFM and AICUBFM.

Frequency sub-band (GHz)	Method					
	IUCBFM			A IUCBFM		
	Number of IUCBFs	CBF construction time (s)	RCS calculation time (s)	Number of IUCBFs	CBF construction time (s)	RCS calculation time (s)
0.1–0.4625	206	0.00	1613.12	74	74.87	529.51
0.4625–0.825	206	0.00	1614.52	91	74.36	646.58
0.825–1.55	206	0.00	1615.23	149	73.14	1028.87
1.55–3.0	206	68.12	1613.88	206	68.21	1615.95

The scattering problem of a PEC sphere with radius of 0.1 sm is considered next. The frequency range starts from 0.2 GHz and terminates at 2 GHz. The discretization in triangular patches is conducted at 3 GHz which leads to 5791 unknowns. The geometry is divided into 8 blocks. In the IUCBFM, 8 plane wave excitations in directions of θ and ϕ are set and 101 IUCBFs retained on each block after the SVD. In the AIUCBFM, the given frequency band is adaptively divided into 3 sub-bands. The broadband RCS (10 frequency sampling points in each sub-band) is obtained by using the IUCBFM and AIUCBFM and shown in Fig. 3. Table 2 separately lists the number of IUCBFs and CPU time of the IUCBFM and AIUCBFM. From Fig. 1 and Table 2, it can be seen that the AIUCBFM can compress more CPU time than the conventional IUCBFM at lower frequency bands, without compromising the accuracy.

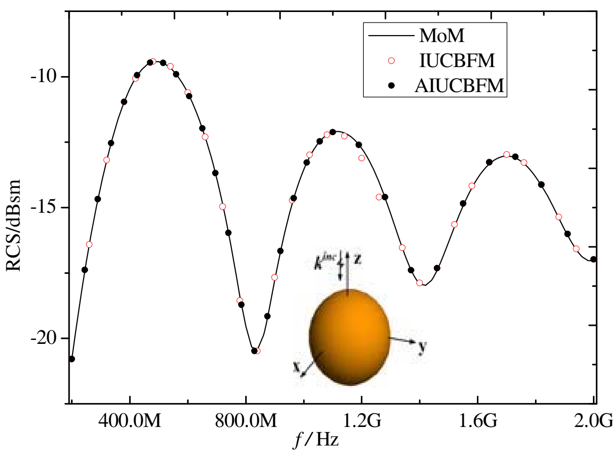

Figure 3. Broadband RCS of the PEC sphere.

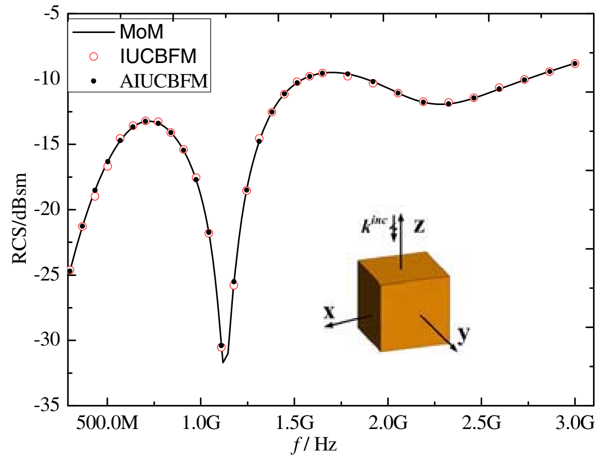

Figure 4. Broadband RCS of the PEC cube.

Table 2. Number of IUCBFs and the CPU time of IUCBFM and AICUBFM.

Frequency sub-band (GHz)	Method					
	IUCBFM			A IUCBFM		
	Number of IUCBFs	CBF construction time (s)	RCS calculation time(s)	Number of IUCBFs	CBF construction time (s)	RCS calculation time (s)
0.2–0.65	809	0.00	7010.21	344	218.23	2130.40
0.65–1.1	809	0.00	7013.25	550	214.75	4159.97
1.1–2.0	809	212.52	7012.18	809	212.91	7018.41

Finally, a PEC cube with a side length of 0.1 m is considered. The results for the problem of scattering over a frequency range from 0.3 GHz to 3 GHz are presented. The geometry is divided into 2379 triangular patches with an average length of $\lambda/10$ at 3 GHz, thus resulting in 6062 unknowns. The geometry is divided into 8 blocks. In the IUCBFM, 8 plane wave excitations in directions of θ and ϕ are set and 94 IUCBFs retained on each block after the SVD. In the AIUCBFM, the given frequency band is adaptively divided into 3 sub-bands. The wideband RCS (10 frequency sampling points in each sub-band) calculated by using the IUCBFM and the AIUCBFM is shown in Fig. 4. The number of IUCBFs and CPU time of the IUCBFM and AIUCBFM are shown in Table 3. As shown in Fig. 4 and Table 3, the AIUCBFM leads to relatively small number of IUCBFs at lower frequencies which results in substantial time-saving without compromising the accuracy.

Table 3. Number of IUCBFs and the CPU time of IUCBFM and AICUBFM.

Frequency sub-band (GHz)	Method					
	IUCBFM			A IUCBFM		
	Number of IUCBFs	CBF construction time (s)	RCS calculation time (s)	Number of IUCBFs	CBF construction time (s)	RCS calculation time (s)
0.3–0.975	754	0.00	7942.58	345	242.74	2571.41
0.975–1.65	754	0.00	7943.53	488	240.47	4283.66
1.65–3.0	754	232.89	7942.27	754	232.59	7948.68

5. CONCLUSION

This paper puts forward an effective numerical method for calculating the wideband RCS of the PEC objects. The AIUCBFM adaptively divides the given frequency band into multiple sub-bands in consideration of the number of the IUCBFs. The adaptive division results in smaller number of IUCBFs at lower frequency band, effectively decreasing the computational complexity at the lower frequency points. The results have demonstrated that the proposed method is able to calculate the wideband RCS more efficiently than the conventional IUCBFM without compromising the accuracy.

ACKNOWLEDGMENT

This work was supported by the National Natural Science Foundation of China under Grant No. 61401003, the Natural Science Foundation of Anhui Provincial Education Department under Grant No. KJ2016A669, and the Natural Science Foundation of Huainan Normal University under Grant No. 2015xj09zd.

REFERENCES

1. Harrington, R. F., *Field Computation by Method of Moments*, IEEE Press, New York, 1992.
2. Coifman, R., V. Rokhlin, and S. Wandzura, "The fast multipole method for the wave equation: A pedestrian prescription," *IEEE Ant. Propag. Mag.*, Vol. 53, No. 3, 7–12, 1993.
3. Song, J. M., C. C. Lu, and W. C. Chew, "Multilevel fast multipole algorithm for electromagnetic scattering by large complex objects," *IEEE Trans. Antennas Propag.*, Vol. 45, No. 10, 1488–1493, 1997.
4. Chen, M., R. S. Chen, and X. Q. Hu, "Augmented MLFMM for analysis of scattering from PEC object with fine structures," *Applied Computational Electromagnetics Society (ACES)Journal*, Vol. 26, No. 5, 418–428, 2011.
5. Bleszynski, E., M. Bleszynski, and T. Jaroszewicz, "Adaptive integral method for solving large-scale electromagnetic scattering and radiation problems," *Radio Sci.*, Vol. 31, No. 5, 1225–1251, 1996.
6. Zhao, K., M. N. Vouvakis, and J.-F. Lee,, "The adaptive cross approximation algorithm for accelerated method of moments computations of EMC," *IEEE Trans. Electromagn. Compat.*, Vol. 47, No. 4, 763–773, 2005.
7. Prakash, V. V. S. and R. Mittra, "Characteristic basis function method: A new technique for efficient solution of method of moments matrix equations," *Microw. Opt. Technol. Lett.*, Vol. 36, No. 2, 95–100, 2003.
8. Lucente, E., A. Monorchio, and R. Mittra, "An iteration free MoM approach based on excitation independent characteristic basis functions for solving large multiscale electromagnetic scattering problems," *IEEE Trans. Antennas Propag.*, Vol. 56, No. 4, 999–1007, 2008.

9. Burke, G. J., "Using model based parameter estimation to increase the efficiency of computing electromagnetic transfer functions," *IEEE Trans. Mag.*, Vol. 25, 2807–2809, 1988.
10. Newman, E. H., "Generation of wide band from the method of moments by interpolating the impedance matrix," *IEEE Trans. Antennas Propag.*, Vol. 36, 1820–1824, 1988.
11. Reddy, C. J., M. D. Deshpande, and C. R. Cockrell, "Fast RCS computation over a frequency band using method of moments in conjunction with asymptotic evaluation technique," *IEEE Trans. Antennas Propag.*, Vol. 46, No. 8, 1229-1233, 1998.
12. Wang, X., S. X. Gong, and J. L. Guo, "Fast and accurate wide-band analysis of antennas mounted on conducting platform using AIM and asymptotic waveform evaluation technique," *IEEE Trans. Antennas Propag.*, Vol. 59, No. 12, 4624–4633, 2011.
13. Sun, Y. F., Y. Du, and Y. Sao, "Fast computation of wideband RCS using characteristic basis function method and asymptotic waveform evaluation technique," *Journal of Electronics (in Chinese)*, Vol. 27, No. 4, 463–467, 2010.
14. Han, G. D., Y. H. Pan, and B. F. He, "Fast analysis for 3D wide-band & wide-angle electromagnetic scattering characteristic by AMCBFM-MBPE," *Journal of Microwaves*, Vol. 25, No. 6, 32–37, 2009.
15. Degiorgi, M., G. Tiberi, and A. Monorchio, "Solution of wide band scattering problems using the characteristic basis function method," *IET Microwaves Antennas and Propagation*, Vol. 6, No. 1, 60–66, 2012.
16. Zhang, M. Y., Y. F. Sun, and Z. G. Wang, "Solutions of broadband RCS using the characteristic basis function method," *IEEE MTTS International Wireless Symposium*, 1–4, Mar. 2015.
17. Nie, W. Y. and Z. G. Wang, "Solution for wide band scattering problems by using the improved ultra-wide band characteristic basis function method," *Progress In Electromagnetics Research Letters*, Vol. 58, 37–43, 2016.
18. Tsang, L., C. E. Mandt, and D. H. Ding, "Monte Carlo simulations of the extinction rate of dense media with randomly distributed dielectric spheres based on solution of Maxwell's equations," *Optics Letters*, Vol. 17, No. 5, 314–316, 1992.
19. Wang, Z. G., Y. F. Sun, and G. H. Wang, "Analysis of electromagnetic scattering from perfect electric conducting targets using improved characteristic basis function method and fast dipole method," *Journal of Electromagnetic Waves and Applications*, Vol. 28, No. 7, 893–902, 2014.